inter.noise 2012
august 19-22
new york city, usa
Quieting the World's Cities

Noise measurements in the near field of a high-performance military jet aircraft[1,2]

Alan T. Wall[a)]
Kent L. Gee[b)]
Tracianne B. Neilsen[c)]
Brigham Young University
Department of Physics and Astronomy
N243 ESC
Provo, UT 84602

Michael M. James[d)]
Kevin A. Bradley[e)]
Sally A. McInerny[f)]
Blue Ridge Research and Consulting LLC
15 W. Walnut St.
Asheville, NC 28804

Published near-field analyses of full-scale jet noise are limited, and the application of observed laboratory scale phenomena to full-scale jets is not well understood. To obtain a greater understanding of the connection between radiated noise and source characteristics in full-scale, heated, supersonic jets produced by military aircraft, acoustical measurements were made in the geometric near field of the jet produced by the installed engine on an F-22A Raptor. In this paper, level-based results are shown, including overall

---

[a)] email: alantwall@gmail.com; Brigham Young University, Provo, UT 84602
[b)] email: kentgee@byu.edu
[c)] email: tbn@byu.edu
[d)] email: michael.james@blueridgeresearch.com
[e)] email: Kevin.Bradley@BlueRidgeResearch.com
[f)] email: sallyannemcinerny@gmail.com

levels, spectral content and how the spectra vary over space. From these results important near-field jet-noise phenomena are identified.

1 INTRODUCTION

The noise radiated from jets on military aircraft is not well understood because characteristics unique to supersonic, high-temperature, full-scale engines have not previously been widely investigated. A connection must be established between turbulent flow structures in a jet and radiated noise in order to understand and improve the impact of noise control measures. Extensive measurements were made in the geometric near field of a high performance military aircraft to characterize the acoustic environment of maintainer personnel, and to provide greater understanding of full scale jet noise phenomena.[1-4] The purpose of this paper is to provide basic analyses of near-field properties, and source characteristics that are inferred from these properties, with a focus on phenomena unique to full-scale jet engine noise.

The majority of today's jet noise studies have been limited to smaller, laboratory-scale tests. Some acoustical data are available for high Mach number flows,[5-8] but test facilities are generally scale, temperature and velocity-limited. Several notable studies have been performed of model-scale jets in the near field,[9-11] and others of full-scale jets in the far field,[12-14] but studies performed in the near field of military-type jets are few.[15] This study addresses some jet noise phenomena observed from measurements made in the geometric near field of the jet produced by an installed engine on an F-22A Raptor.

2 EXPERIMENT OVERVIEW

More than 6000 measurement points and the repetition of the measurement over four engine conditions make this the most extensive near-field measurement of a jet on a high-performance military aircraft to date. This experiment was designed for a near-field acoustical holography analysis,[4,16-19] although holography results are not presented in this paper. This section summarizes the acoustical measurements made in the geometric near field of an F-22A Raptor. First, details about the aircraft, test environment and microphone arrays are presented. Additional details about the experiment are described elsewhere by James *et al.*[1], James and Gee,[2] and Wall *et al.*[3]

2.1 Aircraft and Test Environment

Researchers at Blue Ridge Research and Consulting and Brigham Young University conducted static run-up tests on the Lockheed Martin/Boeing F-22A Raptor. The F-22A has two Pratt & Whitney F119-PW-100 turbofan engines that are each in the 160 kN (35,000 lbf) thrust class. The engine closest to the measurement arrays was cycled through four power conditions: idle, intermediate, military, and full afterburner, while the other engine was held at idle.

During the static run-up measurements the aircraft was tied down in the center of a 24.4 m (80 ft) wide concrete ground run-up pad. Rain-packed dirt was on either side of the pad, making the terrain very flat. Over the short propagation distances in this measurement (<23 m) the effects of temperature fluctuations and wind speeds were determined to be minor. Meteorological trends near the run-up pad were monitored continuously, and all measurements occurred at times that avoided moderate winds and significant temperature lapses.

2.2 Field Array and Reference Array

The field array used in this experiment allowed for a series of dense, large-aperture, two-dimensional measurements of the sound field. The microphones were arranged in 5 rows and 18 columns with 0.15-m (6.0-in) equal spacing. The field array was mounted to an extruded aluminum guide rail for easy mobility and precision placement.

Figure 1 describes the measurement locations relative to the aircraft. In addition to the *x* and *z* coordinates marked on the schematic, the vertical axis is represented by *y*, with a positive direction pointing up. The origin of the coordinate system is on the ground directly below the nozzle exit. Red triangles denote the locations of the array center for each "scan" (see Sec. 2.2). Planes 1 and 2 were measured parallel to the estimated shear layer boundary. Plane 3 was measured parallel to the jet centerline. All measurement planes were located sufficiently far from the flow to render flow-induced noise negligible.

In addition to the three planar measurements, an arc-shaped surface was measured in the transition region from the near to the far field. The arc was centered at a point 5.5 m (18.0 ft) downstream of the nozzle (marked by a green "*x*"), with a radius of 22.9 m (75 .0 ft). The arc center represents an attempt to approximate the location of the dominant noise source region, although it is understood that this region is noncompact and varies as a function of frequency and engine operating conditions.[7] Measurements were made along the arc at six locations in 10° increments from 90° to 140°, and a seventh location at 148°. All polar angles reported in this paper are measured relative to the front of the aircraft (inlet axis) and to the arc center at 5.5 m downstream of the nozzle.

An additional 50 microphones (marked by blue dots in Fig. 1) were placed in a fixed-location array to allow for the generation of coherent field measurements from temporally distinct scans, for the purposes of performing near-field acoustical holography.[4,20] Although holography results are not given here, in this paper the reference array is used to provide overall levels and show spectral variation over a large spatial region in the near field from measurements made simultaneously. The reference microphones were placed on the ground 11.6 m (38.0 ft) from the jet centerline (in the *x* direction) and spaced 0.61 m (2.0 ft) apart. With references on the ground, multipath interference due to ground reflections was avoided.

The sequence of cycling through the four engine conditions and recording data, with the field array and reference microphones in a single fixed location, is referred to as a "scan". Scan locations of the field array are marked by red triangles in Fig. 1. Each measurement plane shown in Fig. 1 was composed of a set of scans made along the length of the jet and at several heights.

3 RESULTS AND DISCUSSION

This section presents several results of the near-field experiment described above, with an emphasis on level-based analyses. Specifically, OASPLs, spectral content and the variation of the spectra over space are examined for subsets of the data. In each subsection, measurement results are presented, followed by a discussion of the corresponding physical phenomena that are important for understanding full-scale jet noise.

3.1 Overall Sound Pressure Levels

In order to characterize the aircraft maintainer environment the OASPLs over the measured spatial aperture are given. Important clues about jet-noise radiation characteristics can be obtained by observing the change in overall radiation patterns as a function of engine condition.

Figure 2 shows OASPLs measured by the field array for afterburner engine conditions. The OASPLs measured by the reference microphones, averaged over several scans, for all four engine-power conditions, are shown in Fig. 3. The directly measured levels, represented by black dots, show a somewhat “noisy” variation in level along the reference array. These local variations are a result of a slight bias in the field-calibrated microphone sensitivities. To correct for this uncertainty in calibration, a set of weighting factors was derived by visual inspection of the variation in the levels of the intermediate case. These resulting factors were then applied to all scans and engine conditions, and the resulting “filtered” results are represented by the solid lines. The dashed lines represent ±1 standard deviation of the OASPL at each location.

The reference microphone array, placed along the ground at a perpendicular distance of 12.0 m (39.5 ft) from the center of the aircraft, was near the 42-ft “foul line” position where aircraft maintainer personnel often stand in relation to the jet on the deck of an aircraft carrier. Figure 3 shows that, at afterburner conditions, there is a 25-m region where the OASPL exceeds 140 dB re 20 μPa, and a 5-m region where the OASPL exceeds 150 dB re 20 μPa. The levels at the head of an aircraft maintainer are expected to be slightly lower, since the measurements here experienced a level boost due to the ground reflection, and were taken 0.76 m closer to the jet than the foul line position.$z \leq 19$ m

The relative locations of maximum-level regions from one measurement plane to the next, shown in Fig. 2, as well as the distinct maximum-level regions in Fig. 3, demonstrate a strong lobing of the overall radiation in the aft direction for military and afterburner conditions. However, two important distinctions between military and afterburner conditions exist in the results. The first is that the maximum region measured along the reference array in Fig. 3 shifts forward two or three meters as engine condition increases from intermediate to afterburner. This corresponds to a forward shift of about 10° and is likely due to an increase in the convective speed of large-scale turbulence structures (see Figs. 2.2.9 and 2.2.10 of reference [21].

The second distinction is that the high-amplitude sound field region within the measurement aperture for afterburner conditions is more spatially compact than that for military conditions, as shown in Fig. 3. Since the measurement aperture is limited to the near field, the exact differences in the principal radiation lobes are unclear. Certainly, a simple difference in how the reference array “slices through” two different lobes of similar shape but different orientation would alter the spatial extent of a maximum region. It is also possible that a change in the nature of the source could lead to a narrower principal lobe at afterburner conditions than at military, but a rigorous directivity analysis is precluded here by the lack of far-field data.

3.2 Spectral Analysis

Turbulent structures within a jet vary greatly in their length and time scales. This manifests itself in the broadband spectra of measured jet noise. In this subsection an examination of the measured spectra and a spatio/spectral analysis of the near field radiation lead to insights regarding the dependence of jet noise characteristics on frequency.

3.2.1 Spectral content

The spectral content in the near field is represented here by the frequency-dependent sound pressure levels (SPLs) measured for all four engine conditions at two key locations within the field. The first, at z = 5.5 m downstream (corresponding to an angle of 90° with respect to the front of the aircraft) is shown in Fig. 4a, and a second at z = 15.2 m downstream (corresponding to 130°) is shown in Fig. 4b. These locations are important because previous studies often indicate that jet noise is composed of two distinct source components: fine-scale turbulence that dominates the sideline radiation, and large-scale turbulence structures that dominate the downstream radiation.[22,23] The one-third-octave SPLs represented by solid lines in Fig. 4 have been averaged over all scans. The dashed lines show ±1 standard deviation of the SPLs at each frequency and engine condition. Data for the upper frequencies of the idle and intermediate conditions are not included because they are contaminated by engine noise components. The legends of Fig. 4 list the mean values and standard deviations of the OASPLs corresponding to each condition.

A comparison of Figs. 4a and 4b indicates that the higher frequencies tend to dominate the noise to the sideline, while lower frequencies dominate in the downstream direction. For example, at z = 5.5 m downstream the maximum frequencies are within the 400-Hz one-third octave band for intermediate engine conditions, the 630-Hz band for military conditions, and the 800-Hz band for afterburner conditions. However, at z = 15.2 m, the maximum-frequency bands are 100 Hz for intermediate, 250 Hz for military, and 125 Hz for afterburner conditions. Note that the spectra for idle engine power at both locations do not have as well defined of a characteristic "haystack" shape; hence it is more difficult to draw conclusions about the dependence of dominant frequencies on location with these data.

The spectral dependence on location is qualitatively consistent with the popular two-source jet-noise model. Schlinker,[5] and Laufer *et al.*[22] were the first to observe that there are two independent sources of jet noise: one source generated by large-scale turbulent structures that radiates preferentially in the aft direction and generates Mach waves, and a source generated by the fine-scale turbulence that dominates to the sideline of the jet. Tam *et al.*[23,24] developed empirically determined similarity spectra to characterize the noise radiated by these two sources for any jet. The application of the two-source similarity spectra to high-power jet noise is under investigation.[25]

It is interesting to compare the spectral shapes shown in Fig. 10 for military and afterburner engine conditions measured at z = 15.2 m. With the increase in power from military to afterburner, high frequencies are boosted by about 3 dB, while low frequencies are boosted by about 8 dB. This is accompanied by a double peak near the dominant frequencies. The double peak is not found in laboratory-scale jet noise, but is observed in other full-scale jet ground run-up measurements.[12,15,26] The lower-frequency spectral peak might, in part, be due to the impingement of the jet flow on the ground as it expands downstream of the nozzle, which is referred to as "scrubbing."[27] However, Greska and Krothapalli,[14] show a double peak in the spectra of an F404-GE-402 jet engine, which was mounted 5.5 m above the ground, which virtually eliminated scrubbing effects. Evidence of a double-peak also appears in flyover measurements of the F-15 ACTIVE Aircraft[28] and in flyover measurements of a military jet by McInerny *et. al*.[29] The presence of this feature in full-scale jet noise merits further study.

3.2.2 Spatial/band-level maps

The spectral variation along the rig planes and the reference array may be used to infer indirectly source characteristics. First, Fig. 5 shows SPL maps of several one-third octave bands measured using the field array at plane 2 (see Fig. 1). Figure 5a contains the SPLs measured at military engine power, and Fig. 5b displays afterburner conditions. The corresponding one-third octave band center frequency in hertz is displayed in the bottom right corner of each map. A color axis that spans 20 dB is used in each map for consistency. Vertical black lines in both figures mark the edges of the regions were all SPLs in the column drop at least 3 dB below the maximum SPL.

Before proceeding to level-based maps for the reference array, some comments about what is readily learned from Fig. 5 are merited. First, as is characteristic of jet noise, both the maps for military and afterburner show that the maximum-radiation region (demarcated by the 3-dB down points) moves upstream and generally becomes more compact as frequency increases. Second, there is also some indication that the location of this dominant region is asymptotically approaching some limit downstream of the nozzle for these conditions. This is supported by the level maps of higher frequencies (not shown). Although this is a field measurement, rather than a source measurement, the upstream movement and spatial constriction of the maximum-level region with increasing frequency agrees, in principle, with Lee and Bridge's[8] phased-array estimates of the dominant aeroacoustic source region in heated model-scale jets.

The rig-based SPL maps in Fig. 5 contain horizontal null regions due to multipath interference effects from reflections off the run-up pad. Although these interference nulls are present in realistic run-up and take-off environments, and can be useful in understanding source characterisics,[30,31] the additional spatial variation of spectral levels due to the presence of a reflecting plane can make examination of spectral trends more difficult. Therefore, it is useful to examine level-based maps measured by the reference array, which was placed on the ground. SPLs as a function of one-third-octave band-center frequency and location in z are displayed in Fig. 6 for military and afterburner engine conditions. The contour lines represent step sizes of 1 dB, and all color axes span a range of 20 dB.

Figure 6 reveals the trend that the region of maximum level in the near field moves upstream and constricts spatially with an increase in frequency for both engine conditions. It also demonstrates further the two-peak phenomenon seen at afterburner and military powers in Fig. 4b. In Fig. 6b, there appears to be two distinct, dominant, spatio/spectral components, or regions of local maximum level. The high-frequency component dominates farther upstream and the low-frequency component dominates in the downstream direction. For the afterburner conditions shown in Fig. 6b, the spectra between $z = 13$ m and $z = 22$ m all contain a local maximum frequency near 125 Hz. However, the local frequency maxima of the second component are spatially dependent. Near $z = 14$ m the dominant frequency is about 250 Hz, but shifts gradually to 800 Hz near $z = 5$ m. The results of military conditions are qualitatively similar in Fig. 6a.

Caution should be used in drawing conclusions about far-field directivity from the spatial maps in Figs. 3 and 5-6, since the measurements were taken in the geometric near field. For example, note that the farthest-aft portion of the arc is only about 8 m from the estimated shear layer location. In addition, although the features are similar, when the angular locations of either the arc or the reference microphones are used, similar features for the afterburner spectra are farther aft by 5-10° relative to far-field F-22A spectra shown previously by Gee *et al.*[12]

4 CONCLUSIONS

Turbulent jets from full-scale engines on military aircraft are some of the largest and most complicated noise sources of interest in aeroacoustics. This paper describes basic results of measurements made in the geometric near field of the jet on an F-22A Raptor. It is shown here that an increase in engine power from military to afterburner conditions results in a forward-shifting of the noise radiation and a possible increased lobing effect. It is also shown that, in the downstream direction, as engine power increases from military to afterburner engine conditions the low-frequency noise components increase much more rapidly than high-frequency components. This is coupled with the occurrence of two distinct maximum regions in the level maps as a function of frequency and location: a low-frequency component that dominates downstream and where the maximum frequency is nearly independent of location, and a high-frequency component that dominates upstream with a location-dependent maximum frequency.

The scope of the measurements made in this experiment provides for a detailed characterization of full-scale jet-noise sources and the near sound field using near-field acoustical holography methods. The extensive measurements should also allow for future beamforming, near-field correlation and coherence, vector acoustic intensity, partial field decomposition and nonlinear shock-formation analyses. These analyses can expand the understanding of high-power jet noise properties in the near field and help to determine important jet-noise source characteristics.

5 ACKNOWLEDGMENTS

The authors gratefully acknowledge funding from the Air Force Research Laboratory through the SBIR program and support through a Cooperative Research and Development Agreement (CRADA) between Blue Ridge Research and Consulting, Brigham Young University, and the Air Force. The authors also recognize the contributions of Micah Downing and Bruce Ikelheimer at Blue Ridge Research and consulting; Michael Gardner and Cole Duke from Brigham Young University; Graystone Design Solutions; National Instruments; G.R.A.S. Sound & Vibration; Dan Santos with the 508 ASW/YF at Hill Air Force Base; Senior Master Sergeant Neil Raben and the 49th Fighter Wing at Holloman Air Force Base; and Richard McKinley, Robert McKinley, and Frank Mobley with the U.S. Air Force Research Laboratory. This research was supported in part by the appointment of Alan Wall to the Student Research Participation Program at U.S. Air Force Research Laboratory, Human Effectiveness Directorate, Warfighter Interface Division, Battlespace Acoustics administered by the Oak Ridge Institute for Science and Education through an interagency agreement between the U.S. Department of Energy and USAFRL. Photographs have been cleared by the 49th Fighter Wing Public Affairs Office at Holloman Air Force Base.

6 REFERENCES

1. M. M. James, K. L. Gee, A. T. Wall, J. M. Downing, K. A. Bradley and S. A. McInerny, "Aircraft jet source noise measurements of a Lockheed Martin F-22 fighter jet using a prototype near-field acoustical holography measurement system," *J. Acoust. Soc. Am.* **127**(3), 1878, (2010).

2. M. M. James and K. L. Gee, "Aircraft Jet Plume Source Noise Mesurement System," *Sound Vib.* **44**(8), 14-17, (2010).

3. A. T. Wall, K. L. Gee, M. M. James, K. A. Bradley, S. A. McInerny and T. B. Neilsen, "Near-field noise measurements of a high-performance military jet aircraft," Noise Control Eng. J., (submitted 2012).

4. A. T. Wall, K. L. Gee, M. D. Gardner, T. B. Neilsen and M. M. James, "Near-field acoustical holography applied to high-performance jet aircraft noise," *Proceedings of Meetings on Acoustics* **9**(1), 040009, (2011).

5. R. H. Schlinker, *Supersonic Jet Noise Experiments* (Ph. D. Dissertation, University of Southern California, Los Angeles, CA, 1975).

6. C. K. W. Tam, "Supersonic jet noise," *Annu. Rev. Fluid Mech.* **27**(1), 17-43, (1995).

7. C. K. W. Tam, N. N. Pastouchenko and R. H. Schlinker, "Noise source distribution in supersonic jets," *J. Sound Vib.* **291**(1-2), 192-201, (2006).

8. S. S. Lee and J. Bridges, "Phased-Array Measurements of Single Flow Hot Jets," AIAA Paper 2005-2842, May 2005.

9. J. C. Yu and D. S. Dosanjh, "Noise Field of a Supersonic Mach 1.5 Cold Model Jet," **51**(5A), 1400-1410, (1972).

10. R. Reba, J. Simonich and R. Schlinker, "Measurement of Source Wave-Packets in High-Speed Jets and Connection to Far-Field Sound," AIAA Paper 2008-2891, May 2008.

11. T. Suzuki and T. Colonius, "Instability waves in a subsonic round jet detected using a near-field phased microphone array," *J. Fluid Mech.* **565**, 197-226, (2006).

12. K. L. Gee, V. W. Sparrow, M. M. James, J. M. Downing, C. M. Hobbs, T. B. Gabrielson and A. A. Atchley, "The role of nonlinear effects in the propagation of noise from high-power jet aircraft," *J. Acoust. Soc. Am.* **123**(6), 4082-4093, (2008).

13. K. Viswanathan, "Does a Model-Scale Nozzle Emit the Same Jet Noise as a Jet Engine?," *AIAA J.* **46**(2), 1715-1737, (2008).

14. B. Greska and A. Krothapalli, "On the Far-Field Propagation of High-Speed Jet Noise," *ASME 2008 Noise Control and Acoustics Division Conference*, (2008).

15. R. H. Schlinker, S. A. Liljenberg, D. R. Polak, K. A. Post, C. T. Chipman and A. M. Stern, "Supersonic Jet Noise Source Characteristics & Propagation: Engine and Model Scale," AIAA Paper 2007-3623, May 2007.

16. M. Lee and J. S. Bolton, "Source characterization of a subsonic jet by using near-field acoustical holography," *J. Acoust. Soc. Am.* **121**(2), 967-977, (2007).

17. A. T. Wall, K. L. Gee, M. M. James and M. D. Gardner, "Application of near-field acoustical holography to high-performance jet aircraft noise," *J. Acoust. Soc. Am.* **127**(3), 1879, (2010).

18. A. T. Wall, K. L. Gee, T. B. Neilsen and M. M. James, "Considerations for near-field acoustical inverse measurements on partially correlated sources," *J. Acoust. Soc. Am.* **128**(4), 2285, (2010).

19. H. Vold, P. N. Shah, J. Davis, P. G. Bremner, D. McLaughlin, P. Morris, J. Veltin and R. McKinley, "High-resolution continuous scan acoustical holography applied to high-speed jet noise," AIAA Paper 2010-3754, June 2010.

20. M. Lee and J. S. Bolton, "Scan-based near-field acoustical holography and partial field decomposition in the presence of noise and source level variation," *J. Acoust. Soc. Am.* **119**(1), 382-393, (2006).

21. S. A. McInerny, G. Lu and S. Olcmen, "Rocket and Jet Mixing Noise, Background and Prediction Procedures", Under Contract UM 03-08-013, August 30, 2004, National Center for Physical Acoustics, University of Mississippi.

22. J. Laufer, R. Schlinker and R. E. Kaplan, "Experiments on Supersonic Jet Noise," *AIAA J.* **14**(4), 489-497, (1976).

23. C. K. W. Tam, K. Viswanathan, K. K. Ahuja and J. Panda, "The sources of jet noise: Experimental evidence," *J. Fluid Mech.* **615**, 253-292, (2008).

24. C. K. W. Tam, M. Golebiowsky and J. M. Seiner, "On the Two Components of Turbulent Mixing Noise from Supersonic Jets," AIAA Paper 96-1716, May 1996.

25. T. B. Neilsen, K. L. Gee, A. T. Wall and M. M. James, "Comparison of near-field military jet aircraft noise with similarity spectra," *J. Acoust. Soc. Am.* **129**(4), 2442, (2011).

26. K. L. Gee, T. B. Gabrielson, A. A. Atchley and V. W. Sparrow, "Preliminary Analysis of Nonlinearity in Military Jet Aircraft Noise Propagation," *AIAA J.* **43**(6), 1398-1401, (2005).

27. D. K. McLaughlin, C.-W. Kuo and D. Papamoschou, "Experiments on the Effect of Ground Reflections on Supersonic Jet Noise," AIAA Paper 2008-22, January 2008.

28. T. D. Norum, D. P. Garber, R. A. Golub, O. L. Santa Maria and J. S. Orme, "Supersonic Jet Exhaust Noise at High Subsonic Flight Speed", NASA/TP-2004-212686, January 2004.

29. S. McInerny, K. L. Gee, M. Dowing and M. James, "Acoustical nonlinearities in aircraft flyover data," AIAA Paper 2007-3654, May 2007.

30. J. Morgan, “Simple-source model of military jet aircraft noise," Senior Thesis, Department of Physics and Astronomy, Brigham Young University, Provo, UT (2011).

31. J. Morgan, K. L. Gee, T. B. Neilsen and A. T. Wall, "A simple-source model of military jet aircraft noise radiation," *Noise Control Eng. J.*, (submitted 2012).

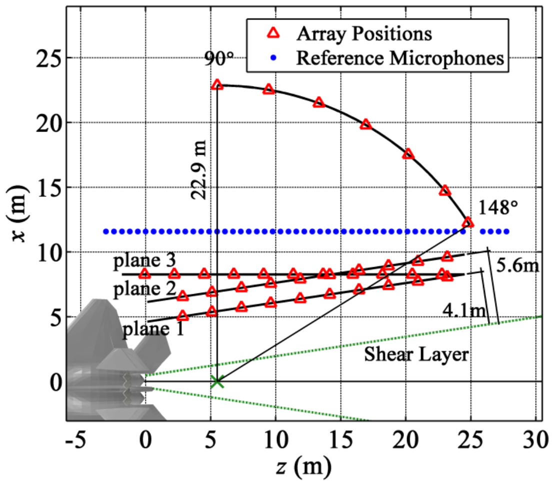

Fig. 1 - Schematic of the measurement locations, relative to the aircraft. The estimated shear layer boundary is marked by green dashed lines, and the green "x" delineates the estimated maximum-noise-source region and the center of the arc.

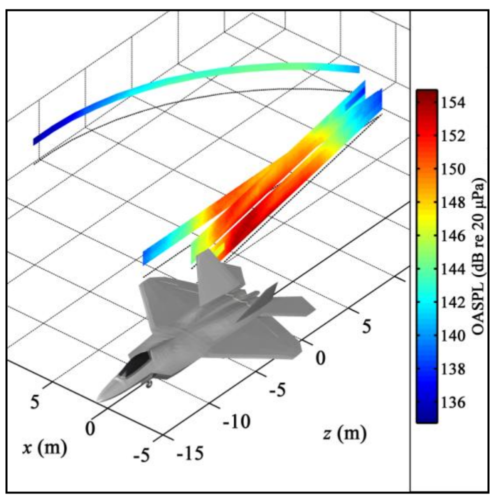

Fig. 2 - OASPLs measured in the geometric near field at afterburner engine conditions. Levels are plotted at their three-dimensional locations.

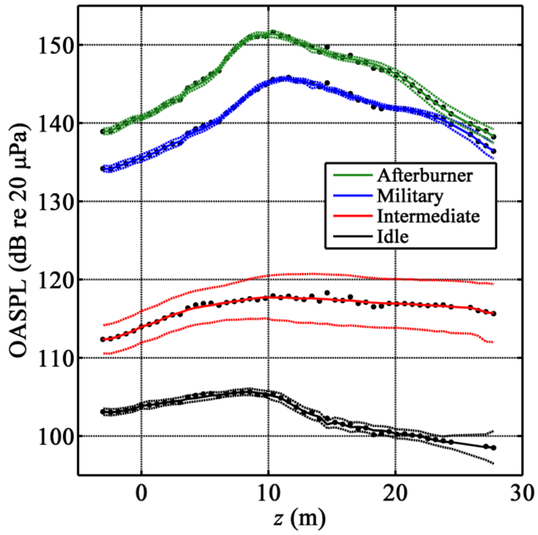

Fig. 3 - OASPLs measured along the ground 12.0 m from the jet centerline by the reference array, for all engine power conditions. Black dots indicate averages of directly measured values and exhibit slight spatial noise due to microphone-sensitivity biases. Smoothed data are shown by a solid colored line, and ± 1 standard deviation over all scans is represented by colored dashed lines.

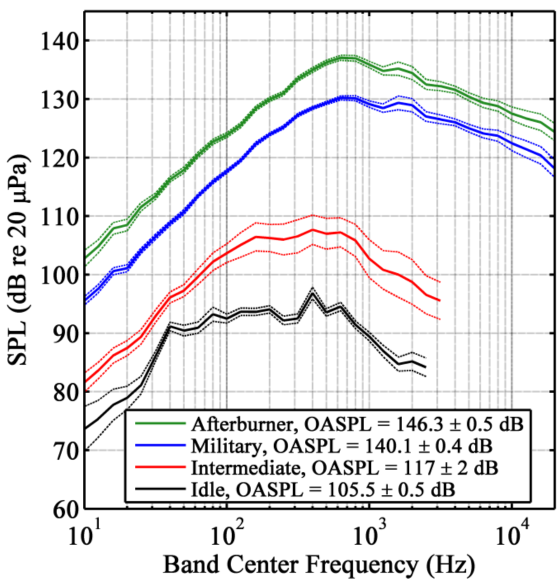

(a)

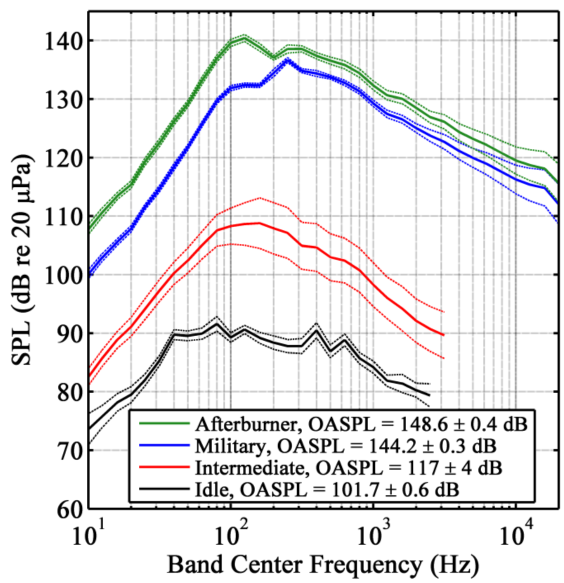

(b)

Fig. 4 – One-third octave spectra measured along the reference array at (a) z = 5.5 m downstream (90°), and (b) z = 15.2 m downstream. Solid lines represent SPL values averaged over all scans. Dashed lines represent ±1 standard deviation. The legend includes the mean values and standard deviations of the respective OASPLs. The upper frequencies of idle and intermediate are not shown due to engine-noise components.

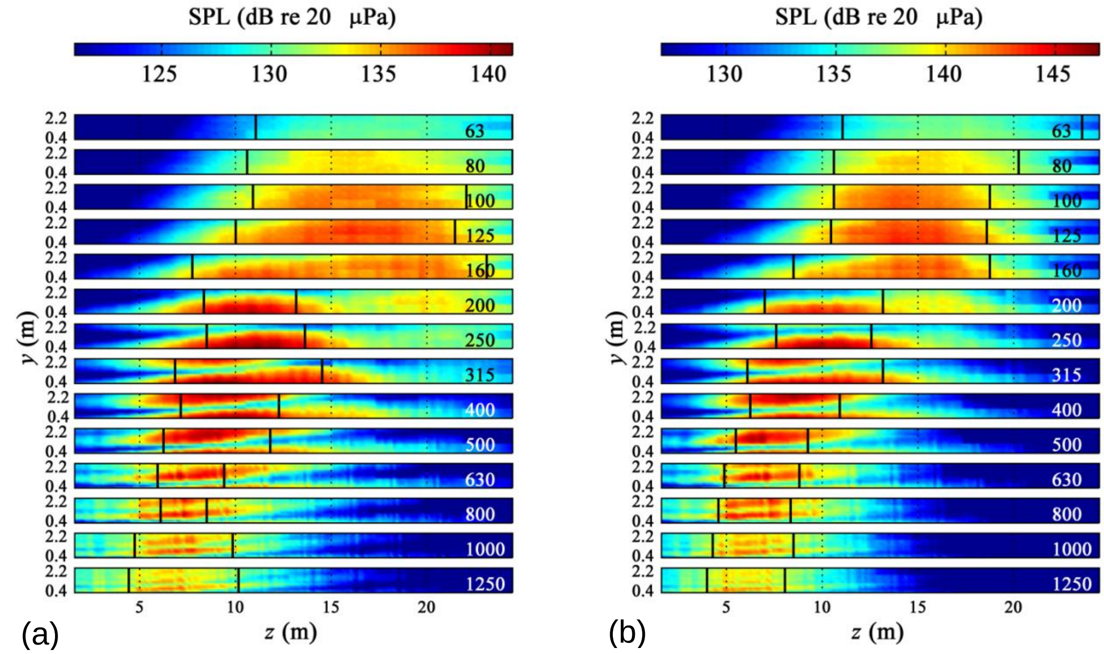

Fig. 5 - SPLs measured at plane 2 for several one-third octave bands at (a) military and (b) afterburner engine power conditions. Vertical black lines indicate the regions where SPLs are within 3 dB of the maximum SPL. The number at the right of each plot is the band center frequency in Hz.

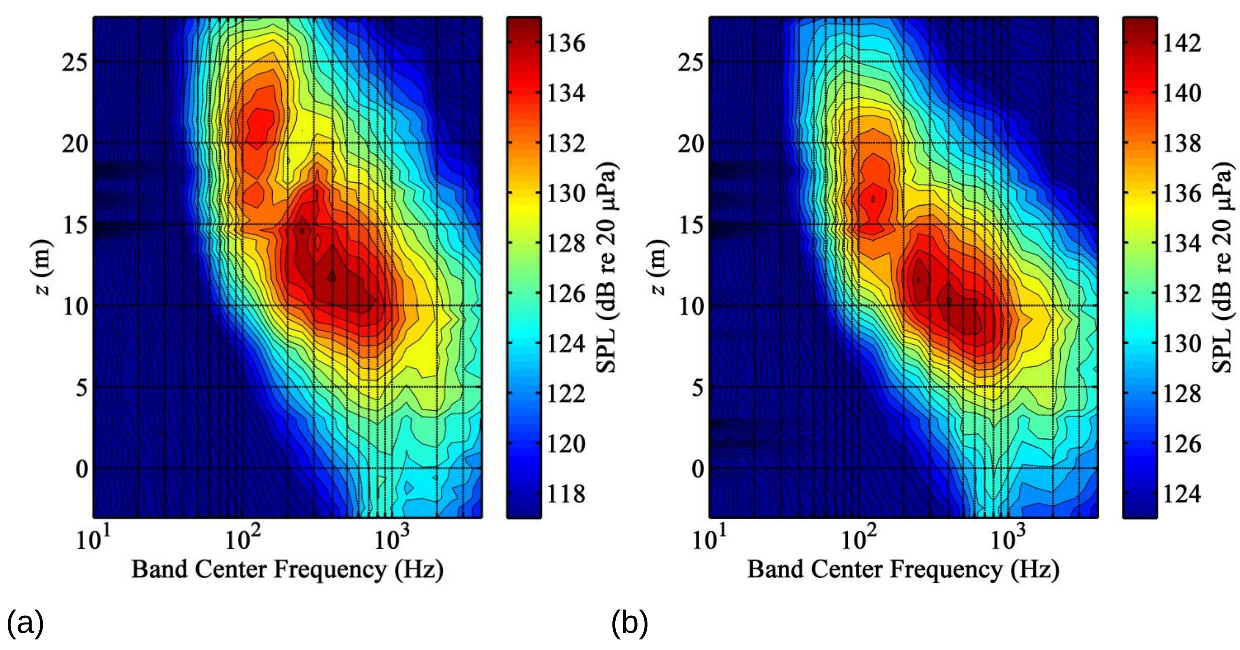

Fig. 6 – One-third octave spectral variation over location along reference array at (a) military and (b) afterburner engine conditions. Each contour line represents a step size of 1dB.